Theoretical and Experimental Study of the Vibrating Fluid Jet Cavities for Large Width Continous Printers

***A. Badea*[*‡], *A. Dunand*[*], *A. Soucemarianadin*[*†] *and C. Carasso*[‡]**
**** Toxot Science & Applications, Cedex, France***
† Laboratoire de Rheologie, Grenoble, France
‡ Universite de Saint Etienne, France

Abstract

Mastering uniform, stable drop generation is paramount for successful continuous inkjet printing. This paper describes a finite element model suited for the simulation of acoustic processes in a 3-dimensional fluid cavity. The model features include provisions for: arbitrary-shaped geometries, influence of transducer displacements and position of fluid inlets and outlets to cite a few. The relevance of our approach is discussed in the light of comparisons with experimental measurements of jet breakoff and possible improvements are suggested.

Introduction

The use of inkjet in large width printing applications is becoming common in industrialized countries where companies have to meet simultaneous constraints such as high throughput, large flexibility, and just in time production. Particular examples are lottery ticket printing or billboard production. Continuous ink jet technology[1] has found a large acceptance in these areas.

For this technology, uniform stable drop generation is required for good image quality. For large width applications, several solutions have been proposed to minimize standing wave effects. These include random noise[2] or travelling wave systems[3] for jet stimulation. The design of our large width printer is based on stacking side by side a number of individual print-modules, each module controlling a limited number of jets[4]. The solution for obtaining a homogeneous stimulation of these stackable modules has been a major part of our research, involving both theoretical and experimental developments.

In the theoretical approach, we use a finite element code for modelling the vibrating behaviour of the fluid cavity[5]. Experimental measurements of jet breakoff are performed in conjunction with computations to verify the effect of the main design parameters on jet breakoff length homogeneity. These parameters include the:

- geometry of the cavity
- number of active transducers
- shape of the stimulating electrical signal

Finally, we demonstrate that our approach contains the relevant controlling parameters and provides a good fit with experimental results.

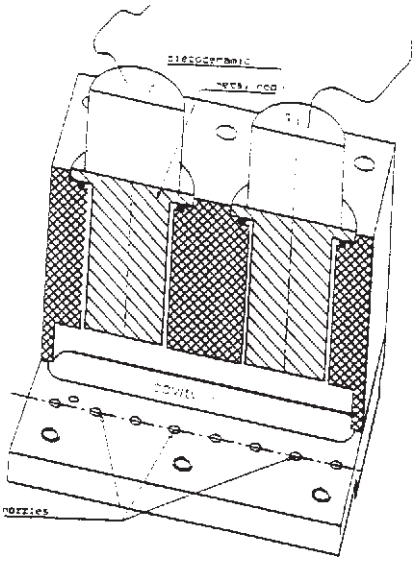

Figure 1. Schematic representation of the droplet generator

Droplet Generator

A multinozzle droplet generator for continuous inkjet printers must meet several requirements[6]. It must deliver a drive perturbation to the nozzle array such that all jets breakoff into uniformly sized and evenly spaced droplets, within a given length interval. It must also be efficient enough to operate at reasonable head-drive voltages under satellite free condition with breakup shape being

Originally published in *Proc. of IS&T's Ninth International Congress on Advances in Non-Impact Printing Technologies*, October 4-8, 1993 in Yokohama, Japan.

similar from jet to jet. The design illustrated in Figure l meets these requirements.

The active elements are either one or two transducers symmetrically aligned with respect to the axis of the droplet generator. Each transducer consists of a metal rod glued to a piezoceramic cylinder and tuned to vibrate longitudinally at the working frequency. To ensure a strong drive to the jets, the distance between the bottom face of the resonators and the nozzles is chosen such that the sound waves generated in the liquid-filled cavity are at near resonance conditions at the operating frequency.

Problem Formulation

Basic Equations

To relate the motion of the fluid to its compression or dilatation, we need a functional relationship between the particle velocity $\vec{v}$ and the instantaneous density ρ. If we consider a volume element dV, the rate with which the mass increases in the volume is $(\partial\rho/\partial t)$ dV. Since the net influx must equal the rate of increase we obtain:

$$\frac{\partial \rho}{\partial t} + div\rho\vec{v} = 0 \tag{1}$$

the equation of continuity. This equation is non-linear. However, if we write $\rho = \rho_0 + \rho'$, use the fact that ρ_0 is a constant in both space and time, and assume that ρ' is very small then (1) becomes:

$$\frac{\partial \rho'}{\partial t} + \rho_0 div\ \vec{v} = 0 \tag{2}$$

which is the linearized continuity equation.

In real fluids, the existence of viscosity and the failure of acoustic processes to be perfectly adiabatic introduce dissipative terms[7]. Here we ignore the effects of viscosity. We then obtain from the Navier-Stokes system, the Euler's equation governing inviscid flows:

$$\frac{\partial \vec{v}}{\partial t} + \vec{v}\cdot(\nabla\vec{v}) = -\frac{\nabla p}{\rho} \tag{3}$$

where ∇ is the gradient operator. It can be simplified if we require $\rho' << 1$ and $|(\vec{v}\cdot\nabla)\vec{v}| << |\partial\vec{v}/\partial t|$ then we obtain assuming $p = p_0 + p'$

$$\frac{\partial \vec{v}}{\partial t} + \frac{\nabla p'}{\rho_0} = 0 \tag{4}$$

This is also called the linear inviscid force equation, valid for acoustic processes of small amplitude.

Using equations (2) and (4) and assuming that we have an adiabatic transformation, one obtains:

$$\frac{\partial^2 \Phi}{\partial^2 t} - c^2\Phi = 0 \tag{5}$$

where Φ is the velocity potential and c the sound velocity of the fluid respectively written as:

$$\vec{v} = \nabla\Phi \quad \text{and} \quad c^2 = \left(\frac{\partial p}{\partial \rho_0}\right) \tag{6}$$

The physical meaning of defining a velocity potential is that the acoustical excitation of an inviscid fluid involves no rotational flow.

Orifice Impedance

The following assumptions:

- velocity of the vibrating body much smaller than the speed of sound,
- the amplitude of oscillations negligible compared to the dimensions of the cavity
- inviscid fluid in the cavity are everywhere satis ied except in the very neighbourhood of the orifice. A classical analysis consists in describing the orifice behaviour by a lumped acoustic impedance, which relates the fluctuating pressures and the volume flow rate[8]:

$$0 = \frac{p_2' - p_1'}{Q / A_0} = \frac{p'}{v_n} - R - iX \tag{7}$$

where $p_2' - p_1'$ is the pressure difference between the inlet and outlet of the orifice, A_0 is the orifice area and Q the flow rate through the orifice, R the orifice resistnace and X the orifice reactance. As a first approximation, we will consider R and X to be independent of flow rate.

Periodic Solutions

The active parts linked to the piezoelectric transducers are assumed to have a known forced periodic displacement of angular frequency ω in the direction normal to the fluid boundary $\vec{n}$:

$$\frac{\partial \Phi}{\partial n} = h_i(x)e^{-i\omega t} \qquad \text{for i = 1, k} \tag{8}$$

We are only interested in the periodic solutions of the problem which lead to seek solutions in the form:

$$\Phi(\vec{x},t) = \Phi_0(\vec{x}).e^{-i\omega t} \tag{9}$$

The linearized lossless wave equation for the propagation of sound in fluids then reduces to the classical Helmholtz equation:

$$\Delta\Phi_0 + \frac{\omega^2}{c^2}\Phi_0 = 0 \tag{10}$$

with the following boundary conditions. The cavity boundaries are rigid, perfectly reflecting the non-active parts of the system:

$$\frac{\partial \Phi_0}{\partial n} = 0 \tag{11}$$

At the orifice, equation (8) reads:

$$\frac{\partial \Phi_0}{\partial n} = h_i(\vec{x}) \text{ for i = 1, k} \tag{12}$$

Taking into account the relationship between p' and ρ'

$$0\,\frac{\partial \Phi_0}{\partial n} - i\rho_0 \omega \Phi_0 = 0 \quad \text{for j = 1, m} \tag{13}$$

If we restrain to the case of a purely imaginary impedance (R = 0) then the above equation becomes:

$$X_j \frac{\partial \Phi_0}{\partial n} + \rho_0 \omega \Phi_0 = 0 \quad \text{for j = 1, m} \tag{14}$$

k represents the total number of transducers and m is the total number of orifices.

Numerical Procedure

Dimensional Analysis

To render more tractable the mathematical problem all the lengths are made dimensionless with respect to the height of the cavity L. Furthermore we define:

$$\varphi = \frac{\Phi_0}{\Phi_{\dim}},\ \Phi_{\dim} = h_i L \text{ and } \frac{X_j}{\rho_0 \omega d} = \frac{l}{d} \tag{15}$$

In this study, we shall choose the orifice aspect ration l/d equal to 1 and $h_1 = h_2 = h$ unless otherwise specified. The relationship between the reactance X_j and other variables as mentioned in (15) is due to Panton and Goldman[8].

The dimensionless equatin for the cavity (Ω') becomes:

$$\Delta\varphi + \left(\frac{\omega L}{c}\right)^2 \varphi = 0 \tag{16}$$

with different boundary conditions give below for:

rigid boundaries (Γ_0'): $$\frac{\partial \Phi}{\partial n'} = 0 \tag{17}$$

moving boundaries (S_i'): $$\frac{\partial \Phi}{\partial n'} = 1 \tag{18}$$

orifices (Γ_0'): $$\frac{\partial \Phi}{\partial n'} + \frac{\rho_0 \omega d}{X_j}\,\frac{L}{d}\,\varphi = 0 \tag{19}$$

Finite Element Method

We use the variational approach to formulate the finite element equations[9]. The calculus of variation is concerned with the determination of a stationary value for a functional which is defined by an appropriate integration of the unknowns over the domain. Let us take $V = \left\{ v \in H^1(\Omega'),\ \frac{\partial v}{\partial n'} = 0 \text{ on } \Gamma_0' \right\}$ to be the space for the test functions. The followings variational formulation is then obtained for $\forall v \in V$:

$$\int_{\Omega'} \nabla\varphi \nabla v dx - \left(\frac{\omega L}{c}\right)^2 \int_{\Omega'} \varphi v dx + \sum_j \frac{\rho_0 \omega L}{X_j} \int_{\Gamma_j'} \varphi v(s) ds = \sum_i \int_{S_i'} h_i v(s) ds \tag{20}$$

The three-dimensional domain is constituted of layers of two-dimensional domains divided into triangular plate elements. The three-dimensional elements are pentahedrons formed with the basis of the triangles. The discretization yields about 7500 brick finite elements domains. The meshing and solving of the set of algebraic equations by the Crout's method are performed using the finite element package MODULEF[10].

Experimental

In order to test the theoretical approach, we have performed breakoff length (BOL) measurements, since theories of jet breakup[11] show that there exists a qualitative relationship between the breakoff distance and the normal pulsating velocity v_n of the jet in the form $\frac{\Delta BOL}{BOL} \approx \frac{\Delta v_n}{v_n}$. The experimental configuration chosen is the eight nozzle droplet generator with two transducers which yielded the best results in terms of BOL homogeneity. The working frequency (f) of the transducers is 83.3 kHz and they can be excited up to 150 volts by separate drivers which also give means to vary the phase. The distance mm and the nozzle diameter is 50 μm. The fluid used is ink with a viscosity η of 5 mPa.s. a surface tension σ of 40. 10-3 N/m and a sound velocity measured by a pusle-echo method[12] equal to 1600 m/s. The jet velocity is kept constant at 20 m/s corresponding to a Reynolds number based on orifice diameter: Re = 200.

The jets' breakoff is studied using the shadowgraph technique. A light emitting diode triggered by the frequency supply of the transducers produces a shadow profile of the jet diameter (the jet is opaque). The considered jet profile is magnified and displayed on a VDU by means of a CCD video camera. Two quantities are measured:

- the perturbation wavelength λ is determined in order to verify the mean velocity U_0 of the jet (using the relation $U_0 = \lambda f$).
- the interruption of the jet shadow nearest to the nozzle is measured to obtain BOL.

In order to determine BOL with an accuracy better than one wavelength, a variable phase shift between the frequency signal and the light peaks allows to stroboscope the jet shadow at different relative times i.e. at different axial locations. The BOL is directly read on a digital display connected to the translation stage holding the droplet generator. The homogeneity between the jets breakoff is defined by the relative deviation in BOL as $(BOL-BOL_{ave})/BOL_{ave}$, where BOL_{ave} is the average breakoff length of all jets.

Results and Discussion

Influence of the Number of Active Transducers on BOL Homogeneity

Figures 2 and 3 give the computed lines of velocity equipotential and their values respectively in the case of one and two transducers for a 9 mm high cavity. Locations of the orifices are indicated by the reference 26 in the figures. Note that in both cases we obtain a plane wave in the middle of the cavity which is deformed as

one approaches the nozzle surface. The velocity equipotentials also show that the homogeneity is better for the two-transducers configuration than for the single one. The former case will be considered as the reference in the following. For the reference case, the absolute values of the orifice potentials lie between 1.9 and 1.5. For the single transducer configuration, absolute values of the orifices potentials lie between 0.5 and 1.2. The double transducer configuraiton is theoretically more efficient.

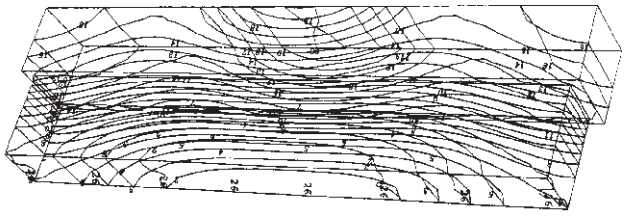

20	—	1.044
19	—	0.9372
18	—	0.8195
17	—	0.7018
16	—	0.5840
15	—	0.4663
14	—	0.3486
13	—	0.2309
12	—	0.1132
11	—	-4.5464E-03
10	—	-0.1223
9	—	-0.2400
8	—	-0.3577
7	—	-0.4754
6	—	-0.5931
5	—	-0.7109
4	—	-0.8286
3	—	-0.9463
2	—	-1.064
1	—	-1.182

Figure 2. Computed contour velocity potential lines in a 9 mm high cavity for a single transducer configuration

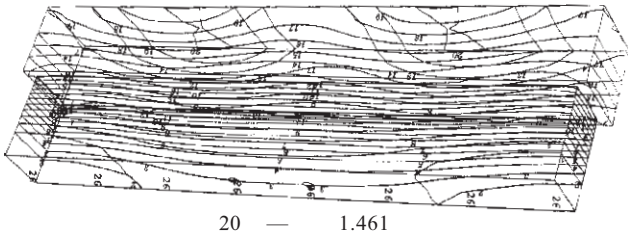

20	—	1.461
19	—	1.300
18	—	1.121
17	—	0.9431
16	—	0.7647
15	—	0.5863
14	—	0.4079
13	—	0.2295
12	—	5.1066E-02
11	—	-0.1273
10	—	-0.3057
9	—	-0.4841
8	—	-0.6625
7	—	-0.8409
6	—	-1.019
5	—	-1.198
4	—	-1.376
3	—	-1.555
2	—	-1.733
1	—	-1.911

Figure 3. Computed contour velocity potential lines in a 9 mm high cavity for a double transducer configuration

As expected from the computed velocity potentials, Figure 4 depicts a large difference in terms of homogeneity for the two above configurations with a dispersion of almost +/- 30% in BOL (it is in fact the relative deviation in pulsating velocity amplitude which is considered) for the single transducer droplet generator. The single transducer droplet generator shows a shorter BOL in the centre jets as compared to the outer jets. This is in contrast to the behaviour obtained with the two transducer configuration.

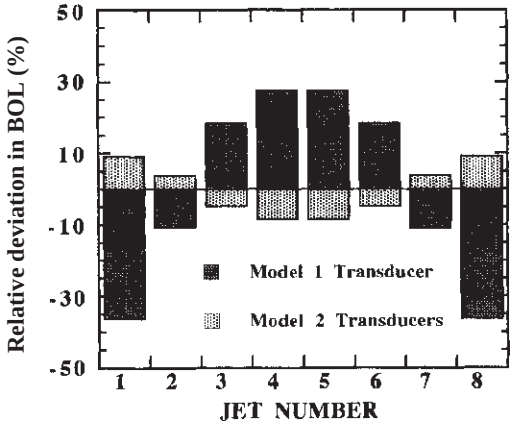

Figure 4. Relative deviation in BOL for single and double transducer configuration

Comparison between Model and Experiement for the Reference Case

The computed relative deviations in jet velocity are shown to agree well with experimental relative deviations in BOL in Figure 5. Note the asymmetric behaviour of the jets observed experimentally. This may be attributed to differences in transducer or nozzle characteristics. The computed and experimental values agree quite well since they are within the experimental scatter.

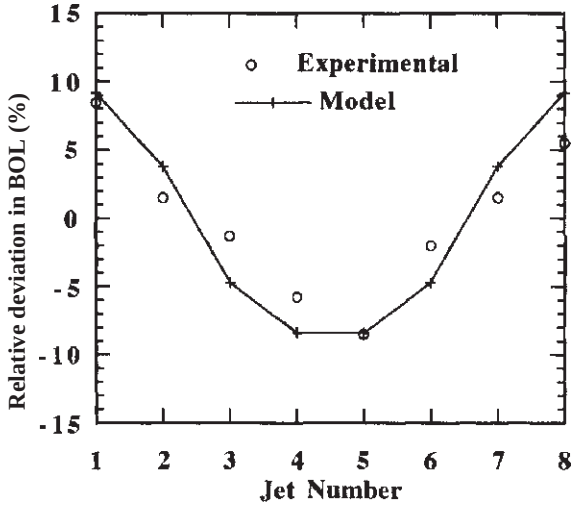

Figure 5. Comparison between model and experiment for the two transducer system

Influence of the Stimulating Electrical Signal on BOL

Figure 6 represents the case where the transducer displacements are out of phase ($h_1 = -h_2$). Here the comparison between computed and experimental results is only fair. The inviscid fluid assumption does perhaps increase the discrepancy. The results illustrate however the possibility to vary breakoff homogeneity with relative phasing between transducers.

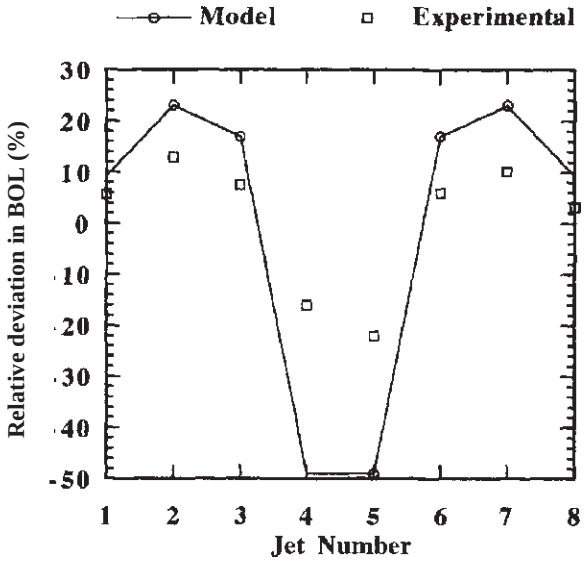

Figure 6. Comparison between model and experiment for out of phase stimulation

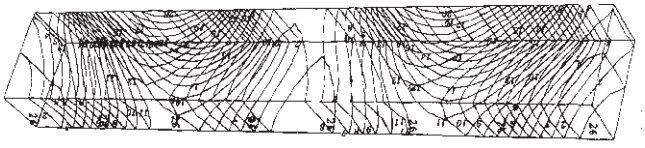

20	—	0.4912
19	—	0.4282
18	—	0.3586
17	—	0.2891
16	—	0.2195
15	—	0.1499
14	—	8.0307E-02
13	—	1.0722E-02
12	—	-5.8863E-02
11	—	-0.1284
10	—	-0.1980
9	—	-0.2676
8	—	-0.3372
7	—	-0.4068
6	—	-0.4764
5	—	-0.5460
4	—	-0.6155
3	—	-0.6851
2	—	-0.7547
1	—	-0.8243

Figure 7. Computed contour velocity potential lines in a 4.9 mm high cavity for a double transducer configuration.

Influence of the Geometry of the Cavity

Figure 7 shows the computed lines of velocity equipotentials and their values for a 4.9 mm (almost λ/4) high cavity. This typical vibrating behaviour of the cavity corresponds to the transverse standing wave pattern which renders quite difficult homogeneous breakoff in large width printers.

Conclusions

In this paper a finite element analysis has been described for simulating acoustic excitation in a 3-dimensional fluid cavity. To demonstrate the relevance of this analysis, it was applied to practical situations found in ink-jet printing. In general, the agreement between predicted values and experimental measurements are fair to good. The model also allows the study of the influence of nozzle aspect ratios and position of fluid inlets and outlets. Planned extensions of this preliminary study are to consider relative phasing between a number of transducers, taking into account more general types of orifice impedance. The final goal is to provide an interactive software capable of sustaining computing and visualization and thus rapid design. This implementation is intended to serve as a step in the direction towards enabling computational experiments as a parallel path to hardware development in ink-jet printing processes.

Acknowledgements

The authors wish to thank the management of Toxot Science & Applications for permission to publish this paper. Part of this work has been performed at Université de Saint-Etienne, under ANRT/CIFRE grant.

References

1. J. L. Johnson “Principles of Non-Impact Printing”, Palatino Press, Irvine (1986).
2. U.S. Patent No. 4,523,202 issued to Burlington Ind.
3. N. Morita, “Multinozzle Drop Generator for Continuous Ink-Jet Printing”, *Electronics and Communications in Japan*, **72** (1989).
4. French patents No. 91 05475 and 91 11151 issued to Toxot Science & Applications.
5. A. Badea, “Modelisation Numérique de Ecoulement Pulsatoire dans un Reservoir d’Imprimante a Jet d’Encre”, Master’s thesis, Université de Saint-Etienne (1991).
6. G. L. Fillmore and D. C. VanLokeren, “A Multinozzle Drop Generator which Produces Uniform Breakup of Continuous Jets”, *IEEE Transactions on Industry Applications*, **20** (1984).
7. L. E. Kinsler, A. R. Frey, A. B. Coppens and J. V. Sanders, “Fundamentals of Acoustics”, Wiley 3rd edition, New York, (1982).
8. R. L. Panton and A. L. Goldman, “Correlation of Non-Linear Orifice Impedance”, *J. Acoust. Soc. Am*. **60** (1976).
9. G. Dhatt and G. Touzot, “Une Présentation de la Méthode des Eléments Finis”, Maloine, Paris (1981).
10. “MODULEF” Finite Element Package issued by the Institut National de Recherche en Informatique et en Automatique (INRIA).
11. H. C. Lee, “Drop Formation in a Liquid Jet”, *IBM J. Res. Develop*., 364-369 (1974).
12. J. Szilar, “Ultrasonic Testing”, Wiley, New York (1982).